Simultaneous Measurement of Electron and Ion Temperatures with Helium-like Argon X-Ray Spectrum

Motoshi GOTO and Shigeru MORITA

National Institute for Fusion Science, Toki 509-5292, Japan

Helium-like argon spectra are measured for plasmas in the Large Helical Device (LHD). The electron temperature T_e derived from the intensity ratio of a dielectronic satellite line ($1 s^2 2p\,^2P_{1/2} - 1s2p^2\,^2D_{3/2}$) to the resonance line ($1 s^2\,^1S_0 - 1s2p\,^1P_1$) is consistent with the central T_e measured with the Thomson scattering method when the electron density n_e has a peaked profile. The ion temperature T_i is simultaneously determined from the Doppler broadening width of the resonance line and an establishment of thermal equilibrium between electrons and ions, i.e., $T_i = T_e$, due to increase of n_e is experimentally confirmed. The density ratio of lithium-like ion to helium-like ion is determined from fitting of the entire spectrum.

1. Introduction

The x-ray spectroscopy has played an important role for the measurement of ion temperature T_i in fusion experiments. In LHD (the Large Helical Device), the temporal development of T_i is routinely measured from the Doppler broadening width of the helium-like resonance line of argon, i.e., Ar XVII $1 s^2\,^1S_0 - 1s2p\,^1P_1$ [1]. Since the ionization potential of helium-like argon ion is rather high (4.12 keV), it is expected that these line emissions are localized in the plasma central region and the obtained result represents the central ion temperature.

In addition to the ion temperature measurement, the helium-like spectrum has found various uses for plasma diagnostics in the plasma core region. The helium-like spectrum here means a group of several emission lines corresponding to the transitions from $n = 2$ levels, where n is the principal quantum number, to the ground state of helium-like ion and numerous satellite lines of lithium-like ion which appear in the same wavelength range as the former. The measurement of electron temperature T_e with the intensity ratio of a dielectronic satellite line to the resonance line is an example of applications which uses the helium-like spectrum [2, 3]. This method utilizes different T_e-dependence of the rate coefficients of the electron impact excitation and dielectronic capture processes. The reliability of the derived parameters inevitably depends on the accuracy of atomic data used in the analyses. Many efforts have been made to improve theoretical calculation methods which produce required atomic data [5].

In TEXTOR, measured spectra were compared with synthetic ones based on newly compiled atomic data and comprehensive consistency was obtained [5]. Similar

comparisons were also made in NSTX [3], where it was demonstrated that the temporal behavior of derived T_e was consistent with the results of the Thomson scattering measurement.

In this paper, temporal behaviors of T_i and T_e are simultaneously derived from the helium-like argon spectra taken from LHD plasmas and their consistency with the change in the background plasma condition is examined.

2. Experimental Setup

The measurement was made for a discharge with magnetic configurations of $R_{ax} = 3.8$ m and $B_{ax} = 2.539$ T, where R_{ax} and B_{ax} are the major radius of the magnetic axis and the magnetic field strength on the magnetic axis, respectively. Figure 1 shows temporal development of the discharge. The plasma was started with electron cyclotron heating (ECH), and was sustained with three neutral beams (NBI). The argon gas-puff was given at $t = 0.3$ s with a 10 ms pulse width. Eight hydrogen pellets were sequentially injected with 40 ms intervals from $t = 0.7$ s.

The line-averaged electron density $\bar{n}_e$ is derived from radial n_e profiles measured with the Thomson scattering method but the absolute values were normalized to the data by interferometer in the initial low density phase. It is clearly seen that $\bar{n}_e$ stepwise increases synchronizing with each pellet injection. The central electron temperature T_{e0} is immediately lowered after the pellet injection is started.

The helium-like argon spectrum was measured with a Johann-type crystal spectrometer which is basically the same as described in detail in Ref. [1] but the radius of curvature of the quartz crystal (2020) has been changed from 3000 mm to 1500 mm. This modification aimed at observing a wider wavelength range in a single measure-
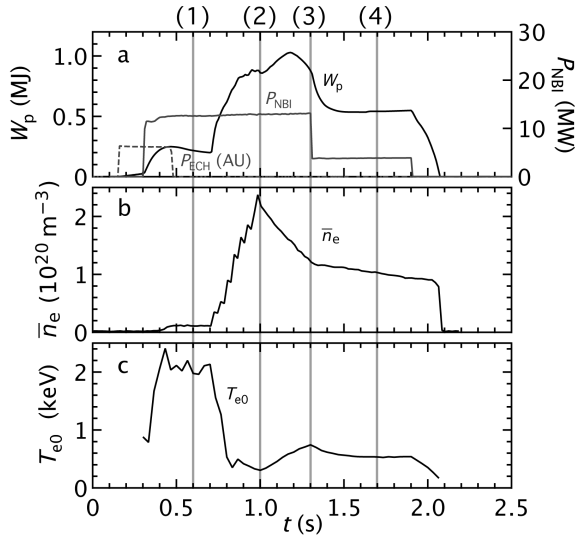
author's e-mail: goto@nifs.ac.jp

Fig. 1   Several parameters for the discharge analyzed here (#69260): (a) the ECH and NBI powers, P_{ECH} and P_{NBI}, respectively, and the stored energy W_p, (b) the line-averaged electron density $\bar{n}_e$, and (c) the central electron temperature T_{e0} by Thomson scattering method. Figure 6 shows the T_e and n_e profiles at the timings (1)-(4).
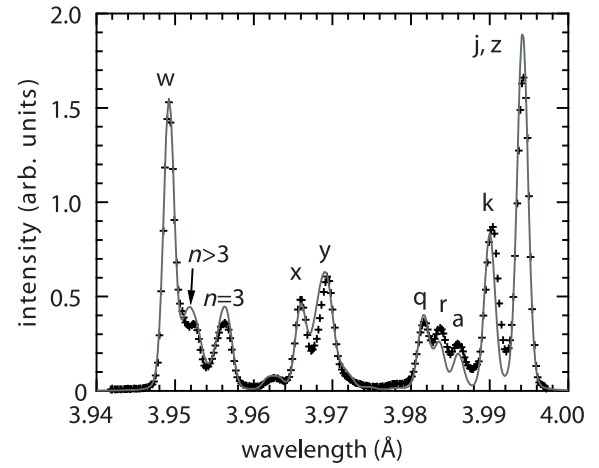

Fig. 2   Example of the measured spectrum made up of the data from two identical LHD discharges #69258 and #69260. The data are summed over from $t = 1.5$ s to 1.7 s. The line notation follows Ref. [4]. The fitting result with $T_e = 525$ eV and $n_{Li}/n_{He} = 0.24$ is shown with the solid line.

ment. The lattice spacing of the crystal is 4.2554 Å, and the Bragg angle and the wavelength dispersion at $\lambda = 3.9492$ Å, which is the wavelength of the helium-like argon resonance line, are 68.1320 degree and 874.049 mm/Å, respectively. A charge coupled device (CCD) was used as the detector. The detection area consists of 1024 pixels (in the direction of wavelength dispersion) times 256 pixels (in the vertical direction to the wavelength dispersion) and the pixel size is 26 μm square. All the data stored in the vertical direction on the detector were binned so that a single spectrum was taken in a single exposure cycle. The temporal resolution was 4 ms.

An example of the measured spectra for the discharge in Fig. 1 is shown with crosses in Fig. 2. Here, the data are summed over a period between $t = 1.5$ s and 1.7 s. The notation of lines follows Gabriel's definition [4]. The lines labeled as w, x, y, and z correspond to the transitions $1 s^2 - 1 s2l$ of helium-like ion and otherwise indicated lines to several representative transitions from doubly excited lithium-like ion, i.e., $1 s^2 2l' - 1 s2l2l'$. The two groups of lines designated as "$n = 3$" and "$n > 3$" correspond to the transitions $1 s^2 nl' - 1 s2lnl'$ with $n = 3$ and $n > 3$, respectively.

It should be here noted that the detector horizontal length (1024×26 μm) is insufficient to get the entire spectrum in Fig. 2 with a single discharge. The spectrum in Fig. 2 is made up of the data from two successive discharges which are almost identical. In the first measurement the wavelength range involving the w to y lines was observed and in the subsequent discharge the detector position was shifted so that the observable wavelength range covered the y to z lines. Since the intensities of the y line

observed in the both discharges are found to be slightly different, the amplitude of the entire spectrum in the second measurement is normalized to that in the first measurement at the y line. The points in Fig. 2 represent the signal counts summed every eight horizontal pixels.

3. Model Calculation

We first focus on the line intensity ratio of the k to w lines which is known to have a strong T_e-dependence [3]. Figure 3 shows a part of the energy level diagram of argon ion relevant to those lines. The upper level of the w line $1s2p\,^1P_1$, which is here also denoted as w, is assumed to be in corona equilibrium, namely, its relative population to that of the ground state is determined so that the excitation from the ground state $1 s^2\,^1S_0$ and the radiative deexcitation to the ground state are balanced. The validity of this assumption has been confirmed in the range of $n_e < 10^{21}$ m^{-3} by calculations with a collisional-radiative model [5].

In this case the populations of the ground state and the w level, n_g and n_w, respectively, should satisfy the equation

$$C_w n_g n_e = A_w n_w, \tag{1}$$

where C_w is the excitation rate coefficient by electron impacts from the ground state to the w level and A_w is the spontaneous radiative transition probability from the w level to the ground state. The right-hand-side of Eq. (1) is nothing less than the intensity or the photon emission rate of the w line.

The upper level of the k line, which is here also denoted as k, is the doubly excited state of lithium-like ion $1s2p^2\,^2D_{3/2}$. The k level is mainly populated through dielectronic captures by the ground state helium-like ion. This process is indicated with an arrow labeled as r_d in
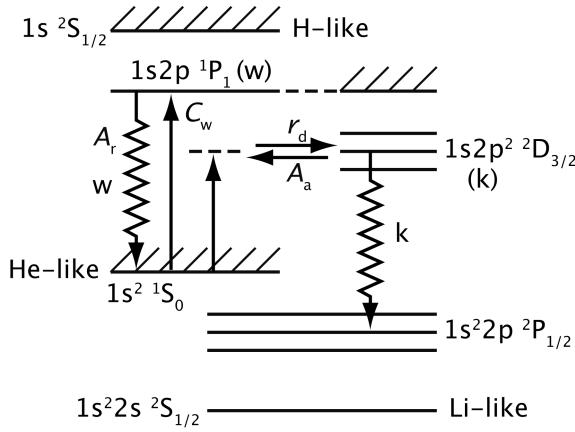
Fig. 3   Schematic energy level diagram relevant to the w and k lines of helium-like and lithium-like ions.

Fig. 4 T_e-dependence of (a) the rate coefficients C_w and r_d and (b) intensity ratios between helium-like lines k/w, x/w, y/w, and z/w.

Fig. 3. The dominant population outflow processes are the autoionization and radiative decay to the singly excited level $1s^2 2p\,^2P_{1/2}$. The latter process is called the stabilizing transition. The k level population, n_k, is determined so that these processes are balanced as

$$n_g n_e r_d = n_k (A_r + A_a), \qquad (2)$$

where r_d is the rate coefficient of the dielectronic capture, and A_r and A_a are the probability for the stabilizing transition and the autoionization, respectively.

Since the dielectronic capture is the reverse process of the autoionization, the quantities r_d and A_a should satisfy the detailed balance equation under thermodynamic equilibrium as

$$\left[n_g n_e r_d = n_k A_a \right]_E, \qquad (3)$$

where $[\cdots]_E$ indicates the condition of thermodynamic equilibrium. The rate coefficient r_d is then expressed as

$$r_d = \left[\frac{n_k}{n_g n_e} \right]_E A_a = Z_k A_a, \qquad (4)$$

where

$$Z_k = \frac{g_k}{2g_g} \left(\frac{h^2}{2\pi m k T_e} \right)^{3/2} \exp\left(-\frac{\chi_{gk}}{kT_e} \right), \qquad (5)$$

is the Saha-Boltzmann coefficient. Here, g_g and g_k are the statistical weight of the helium-like ground state and the level k, respectively, χ_{gk} is the energy level difference between these levels, and h, m, and k are the Planck constant, electron mass, and Boltzmann constant, respectively. Substituting Eq. (4) into Eq. (2) one obtains

$$n_k = \frac{A_a}{A_r + A_a} Z_k n_e n_g. \qquad (6)$$

The k line intensity is understood as $n_k A_r$ and the k to w intensity ratio I_k/I_w is now expressed as

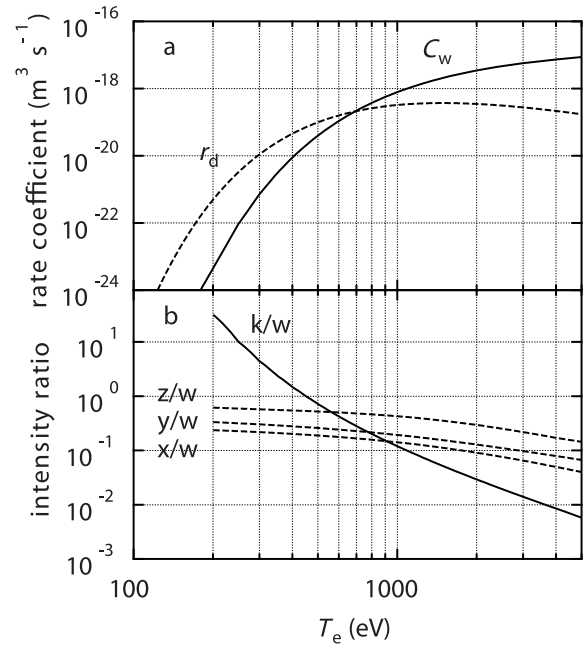$$\frac{I_k}{I_w} = \frac{A_r A_a Z_k}{C_w (A_r + A_a)}. \qquad (7)$$

Figure 4 shows the T_e-dependence of C_w and r_d (a) and I_k/I_w (b). The values C_w, A_r, and A_a are taken from Ref. [5]. The strong T_e-dependence in I_k/I_w stems from the different T_e-dependence between C_w and r_d. Intensities of other helium-like ion lines, x, y, and z, can be obtained from a relation similar to Eq. (1). Figure 4 also shows the intensity ratios of x, y, and z lines to the w line. The advantage of using the k to w ratio for the T_e measurement as compared to using other line ratios is clearly seen.

4. Results and Discussion

The intensities of the w and k lines are derived from the measured spectra: each line profile is fitted with a Gaussian function and its intensity is obtained as its integral. Figure 5 shows (a) the temporal development of the measured I_k/I_w and (b) T_e derived from the measured I_k/I_w and the theoretical data in Fig. 4 (b). The central electron temperature T_{e0} measured with the Thomson scattering method is also shown in the same figure with the dashed line. The discrepancy between the two results is large in the initial phase of the discharge ($t < 0.7$ s) and after starting the pellet injection both values immediately become to coincide with each other.

The disagreement between the two measurements in the initial phase could be ascribed to the fact that the present measurement is based on the line-integral observation. Figure 6 shows the radial profiles of T_e and n_e measured with the Thomson scattering method at the timings indicated with the vertical grey lines in Fig. 1. In the initial low density phase T_e is high enough to produce helium-like ions even in the edge region. Since n_e profile is hollow, the
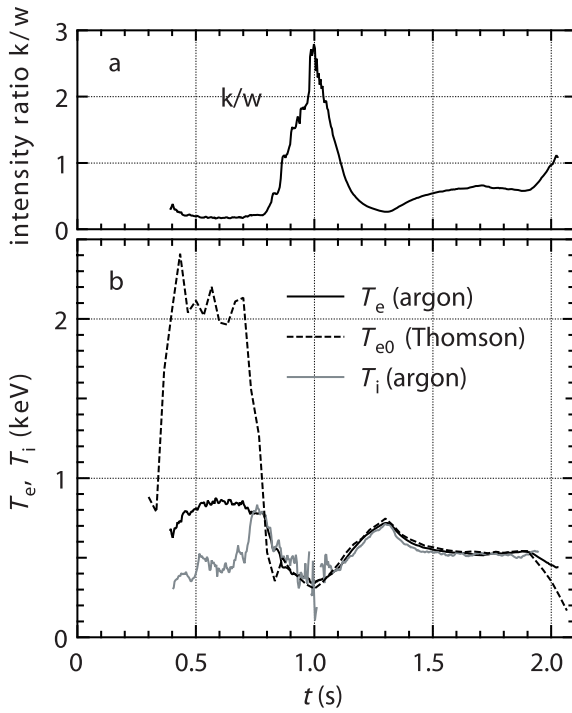
Fig. 5 Measured intensity ratio of the k and w lines for the discharge in Fig. 1 (a) and T_e derived from the k/w ratio, central T_e, T_{e0}, with Thomson scattering, and T_i from Doppler broadening of the w line (b).

Fig. 6 Radial profiles of T_e and n_e measured with the Thomson scattering method at different four stages ((1)-(4)) of the discharge in Fig. 1.

profile of helium-like ion density should be broad. In the T_e range higher than 1 keV the production rate of w level increases with T_e while that of k level is almost constant as seen in Fig. 4. Provided helium-like ion has a flat density profile, the w line emissivity would be peaked at the plasma center while the k line would have a hollow profile. Consequently, the radial location of dominant w line emission could be different from that of dominant k line emission. If that is the case, the actual T_e at the location of dominant w line emission should be higher than the value derived here.

After starting the pellet injection n_e is peaked at the plasma center and T_e is rather low in the entire region. Such characteristics, namely, peaked n_e and flat T_e profiles, are sustained until the end of discharge although the absolute values are dynamically changed. Since the observed spectrum is expected to be dominated by line emissions in the central region, the derived T_e can be regarded as that at the plasma center. As seen in Fig. 5, the present result shows a good consistency with the Thomson's data in this period, and the reliability of the present method is confirmed.

The ion temperature can be, in principle, derived from the Doppler broadening profile of an appropriate emission line, e.g., of the w line. However, since the measured line profile is generally a convolution of the instrumental function and the Doppler profile, a deconvolution of the measured line profile into two components is necessary to de-
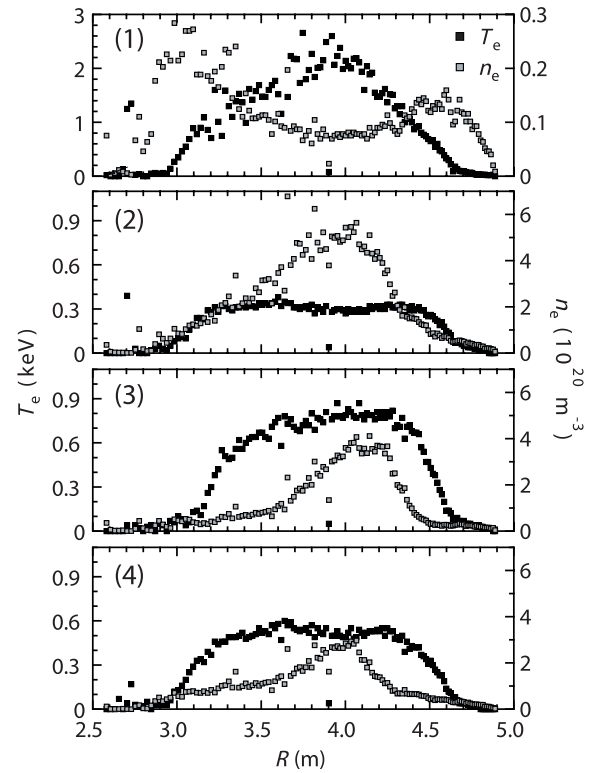
termine T_i.

The instrumental function, which is here approximated with a Gaussian function and represented by its width w_{inst}, is evaluated as follows. When the density is so high that equilibrium between the electron and ion temperatures is expected, namely, $T_i = T_e$, the Doppler (Gaussian) width w_D is estimated from the derived T_e. The instrumental width w_{inst} can then be estimated from the relationship

$$w_{obs}^2 = w_D^2 + w_{inst}^2, \qquad (8)$$

where w_{obs} is the observed line width. Here, w_{inst} for the w line at $t = 1.7$ s is determined and thereby T_i in the entire discharge time is derived. The relation between w_{obs} and w_{inst} at $t = 1.7$ s is shown in Fig. 7 and the derived T_i is shown in Fig. 5 (b) with the gray solid line.

It is noticeable that the derived T_i is lower than T_e determined from the line intensity ratios in the period before the pellet injection is started. Since T_i is determined from the w line profile, the obtained T_i is that at the location of dominant w line emission though the detailed emission location distribution is unclear. On the other hand, it has been pointed out in the foregoing discussion that T_e at the location of dominant w line emission should be higher than the derived value owing to the problem of the line-integral measurement. Therefore, the discrepancy between T_e and T_i as seen in Fig. 5 (b) could be actually even larger. This
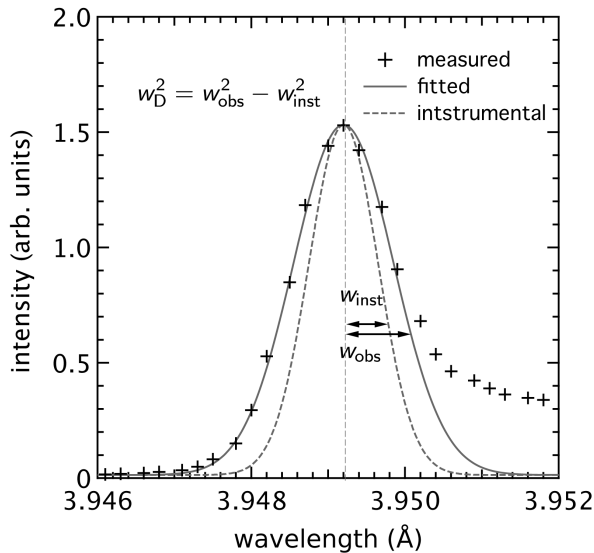
Fig. 7 Measured profile of the w line and instrumental width evaluated at $t = 1.7\,\text{s}$.

result indicates that the thermal equilibrium between electrons and ions has yet to be established at such locations. When n_e is increased due to injection of pellets, the two temperatures instantly coincide with each other and show an almost identical temporal development until the end of discharge.

Finally, density ratios among different charge state ions are considered with the help of emission lines other than w and k. Generally, the line intensity can be separated into three components which are respectively proportional to the densities of helium-like, hydrogen-like, and lithium-like ions. The first component is what we have considered so far. The term proportional to the hydrogen-like ion is the so-called recombining plasma component which contributes to the line intensities of singly excited helium-like ion. A part of satellite lines is from the doubly excited lithium-like ions which are mainly populated through inner-shell excitation of the ground state. Their intensity thus reflects the ion abundance of the lithium-like ion.

We take the spectrum in Fig. 2 as an example and fit it with theoretical calculations to determine relative densities of different charge state ions. The synthetic spectrum is expressed as a linear combination of three components as mentioned above. The individual line emission coefficients are calculated with the atomic data recently compiled by Marchuk [5], where T_e is fixed at 525 eV as derived from the k to w line ratio. This is justified by the fact that the upper levels of the w and k lines are predominantly populated from the helium-like ion and the influence of other charge state ions is small. Every line component is given the same Gaussian profile as evaluated for the w line. The ion density ratios are adjusted so as to have the best consistency between the measured and synthetic spectra. The fitting result indicates that the hydrogen-like ion density is negligibly small and the density ratio of lithium-like to helium-like ions is 0.24. Figure 2 shows the fitted spectrum with the solid line. The disagreement between the two results can most likely be ascribed to the fact that the measurement is based on the line-integral observation while the spectrum is fitted with a single set of parameters. For a further detailed comparison radial profile measurements would be necessary.

From all these results shown here, one may say that the T_e measurement technique with helium-like ion spectrum has arrived at the level for a practical use as well as the T_i measurement. Since Ref. [5] claims that the uncertainty in the atomic data is 4% for C_w and 7% for r_d, the derived T_e values should have the similar degree of uncertainty. In the present measurement, however, the actual uncertainty of the obtained results originates in the problem that the dominant radiation location is unclear. This may be solved if higher-z ions are used so that the dominant radiation is certainly located at the plasma center.

Acknowledgements

[1] S. Morita *et al.*, Rev. Sci. Instrum. **74**, 2375 (2003).
[2] M. Bitter, Phys. Rev. Lett. **43**, 129 (1979).
[3] M. Bitter, Phys. Rev. Lett. **91**, 265001 (2003).
[4] A.H. Gabriel, Mon. Not. R. astr. Soc. **160**, 99 (1972).
[5] O. Marchuk, *Ph. D. thesis* (2004).